

Cite this article as: Marin-Cuartas M, Zhu Y, Imbrie-Moore AM, Park MH, Wilkerson RJ, Leipzig M *et al.* Biomechanical engineering analysis of an acute papillary muscle rupture disease model using an innovative 3D-printed left heart simulator. *Interact CardioVasc Thorac Surg* 2022;34:822–30.

# Biomechanical engineering analysis of an acute papillary muscle rupture disease model using an innovative 3D-printed left heart simulator

Mateo Marin-Cuartas <sup>a,b</sup>, Yuanjia Zhu <sup>a,c</sup>, Annabel M. Imbrie-Moore<sup>a,d</sup>, Matthew H. Park<sup>a,d</sup>, Robert J. Wilkerson<sup>a</sup>, Matthew Leipzig<sup>a</sup>, Pearly K. Pandya<sup>a,d</sup>, Michael J. Paulsen<sup>a</sup>, Michael A. Borger <sup>b</sup> and Y. Joseph Woo<sup>a,c,\*</sup>

<sup>a</sup> Department of Cardiothoracic Surgery, Stanford University, Stanford, CA, USA

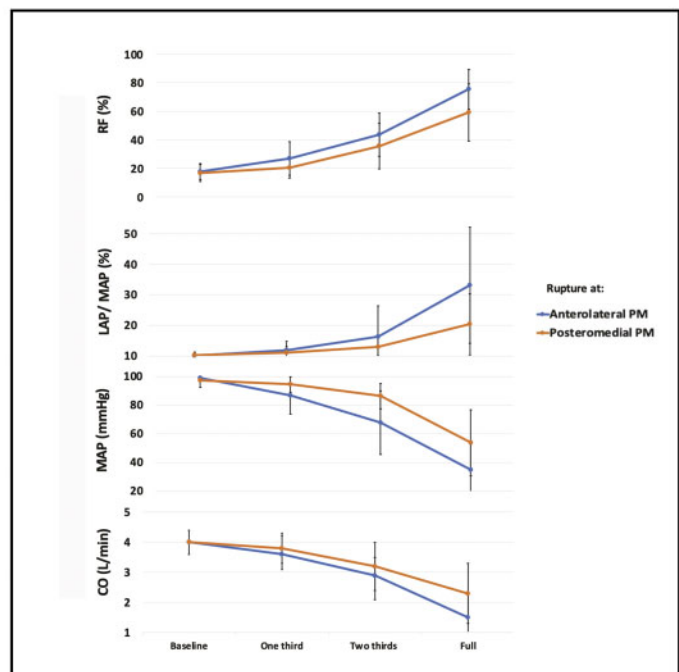
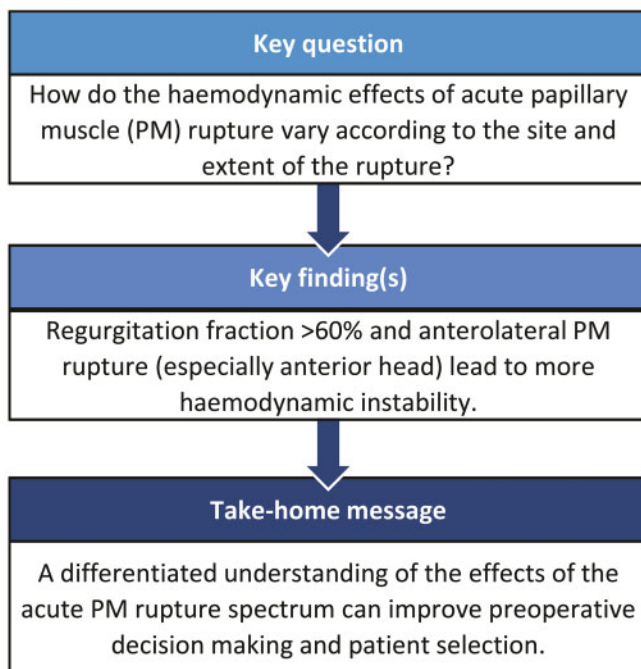
<sup>b</sup> University Department of Cardiac Surgery, Leipzig Heart Center, Leipzig, Germany

<sup>c</sup> Department of Bioengineering, Stanford University, Stanford, CA, USA

<sup>d</sup> Department of Mechanical Engineering, Stanford University, Stanford, CA, USA

\* Corresponding author. Department of Cardiothoracic Surgery, Stanford University School of Medicine, Falk Cardiovascular Research Center, 300 Pasteur Drive, Stanford, CA 94305, USA. Tel: +1-650-725-3828; fax: +1-650-725-3846; e-mail: joswoo@stanford.edu (Y.J. Woo).

Received 15 November 2021; accepted 8 December 2021



## Abstract

**OBJECTIVES:** The severity of acute papillary muscle (PM) rupture varies according to the extent and site of the rupture. However, the haemodynamic effects of different rupture variations are still poorly understood. Using a novel *ex vivo* model, we sought to study acute PM rupture to improve clinical management.

Presented at the 35th Annual Meeting of the European Association for Cardio-Thoracic Surgery, Barcelona, Spain, 13–16 October 2021.

© The Author(s) 2022. Published by Oxford University Press on behalf of the European Association for Cardio-Thoracic Surgery.

This is an Open Access article distributed under the terms of the Creative Commons Attribution-NonCommercial License (<https://creativecommons.org/licenses/by-nc/4.0/>), which permits non-commercial re-use, distribution, and reproduction in any medium, provided the original work is properly cited. For commercial re-use, please contact [journals.permissions@oup.com](mailto:journals.permissions@oup.com)

**METHODS:** Using porcine mitral valves ( $n = 32$ ) mounted within an *ex vivo* left heart simulator, PM rupture was simulated. The mitral valve was divided into quadrants for analysis according to the PM heads. Acute PM rupture was simulated by incrementally cutting from 1/3 to the total number of chordae arising from 1 PM head of interest. Haemodynamic parameters were measured.

**RESULTS:** Rupture  $>2/3$  of the chordae from 1 given PM head or regurgitation fraction  $>60\%$  led to markedly deteriorated haemodynamics. Rupture at the anterolateral PM had a stronger negative effect on haemodynamics than rupture at the posteromedial PM. Rupture occurring at the anterior head of the anterolateral PM led to more marked haemodynamic instability than rupture occurring at the other PM heads.

**CONCLUSIONS:** The haemodynamic effects of acute PM rupture vary considerably according to the site and extent of the rupture. Rupture of  $\leq 2/3$  of chordae from 1 PM head or rupture at the posteromedial PM lead to less marked haemodynamics effects, suggesting a higher likelihood of tolerating surgery. Rupture at the anterolateral PM, specifically the anterior head, rupture of  $>2/3$  of chordae from 1 PM head or regurgitation fraction  $>60\%$  led to marked haemodynamic instability, suggesting the potential benefit from bridging strategies prior to surgery.

**Keywords:** Papillary muscle rupture • Mitral regurgitation • *Ex vivo* model

#### ABBREVIATIONS

CO	Cardiac output
CS	Cardiogenic shock
LAP	Left atrial pressure
LHS	Left heart simulator
MAP	Mean arterial pressure
MCS	Mechanical circulatory support
MI	Myocardial infarction
MR	Mitral regurgitation
MV	Mitral valve
PM	Papillary muscle
RF	Regurgitation fraction

## INTRODUCTION

Acute papillary muscle (PM) rupture is a mechanical complication that leads to severe mitral regurgitation (MR), cardiogenic shock (CS) and acute pulmonary oedema [1]. It is frequently associated with poor outcomes [2–4]. Myocardial infarction (MI) is the most frequent aetiology, most commonly due to occlusion of the right coronary artery [1–3]. The reported incidence of acute PM rupture following MI ranges from 0.25% to 5% [1, 5–7]. It can also occur following severe infective endocarditis or after blunt chest trauma. Acute PM rupture is usually identified with bedside transthoracic or transoesophageal echocardiography [1–4]. Other imaging modalities such as cardiac computed tomography or magnetic resonance usually are not feasible because of the haemodynamic compromise of these patients. A substantial increase in the number of patients presenting with PM rupture has been observed during the current corona virus disease (COVID-19) pandemic due to delayed presentation and management of MI [8, 9]. Despite the increasing observed frequency of PM rupture, the different rupture variations according to the extent and site of rupture are still poorly described and understood.

Even though PM rupture is generally classified as a surgical emergency, given the current lack of evidence on patient selection and management strategies, the correct timing and strategy for surgical intervention are uncertain. Moreover, clinical practice shows that not all patients with PM rupture present with the same severity of haemodynamic compromise. The influence on the clinical presentation of the extent and site of the rupture is still poorly described and understood. Hence, the most effective

haemodynamic stabilization and/or bridging options are uncertain and are mainly decided on a case-to-case basis. Some groups prefer to implant temporary mechanical circulatory support (MCS) before surgery and wait until haemodynamic improvement and consolidation of the infarction zone occur to avoid friable infarcted tissue that makes surgery challenging [10–12]. Alternatively, there are reports of provisional transcatheter edge-to-edge mitral leaflet clipping as a bridging strategy to delay surgery until haemodynamic stabilization is achieved [13, 14]. Other surgeons tend to operate early without bridging strategies to correct the severe MR and revascularize the affected surrounding myocardium as soon as possible [15]. These treatment options are solely based on clinical experience but miss a detailed understanding of the disease's haemodynamical and pathophysiological behaviour. A better understanding of the disease and its various presentations can improve preoperative decision-making, patient selection and surgical planning, thus improving clinical outcomes.

*Ex vivo* simulation of acute PM rupture may provide insights into all these critical aspects. In addition, *ex vivo* simulations are a safe, reliable and reproducible method to analyse acute PM rupture. Its results can be effectively translated into clinical practice, possibly improving the disease's management and outcomes without risking human lives.

This experimental research aims to simulate and study a disease model of acute PM rupture using a left heart simulator (LHS) to improve our understanding and clinical management of the disease based on comprehensive haemodynamic analyses according to the location and extent of the PM rupture.

## MATERIALS AND METHODS

### Ethical statement

No ethics committee approval is required since no human nor animal individuals are involved in this *ex vivo* experimental setup.

### Data availability statement

All relevant data are provided within the manuscript. Additional details can be provided upon request by contacting the corresponding author.

## Left heart simulator

A 3D-printed, custom, modular LHS (Fig. 1) was used as a testing platform to simulate acute PM rupture [16–24]. A 3D printer (Carbon 3D, Redwood City, CA, USA) was used to prototype a modular left heart (left atrium and ventricle) and was mounted to a pulsatile linear piston pump (ViVistro Superpump; ViVistro Labs, Victoria, BC, Canada). This system is equipped with pressure and flow sensors, while compliance chambers generate physiological pressure and flow profiles. A 29-mm mechanical aortic valve (St. Jude Regent, Abbott Vascular, Lake Bluff, IL, USA) was used in the aortic position. The reference valve in the mitral position, used for tuning and calibrating the system, was a 28-mm leak-less disc valve (ViVistro). With this valve, the system was tuned to generate a cardiac output (CO) of 5 l/min with a mean arterial pressure

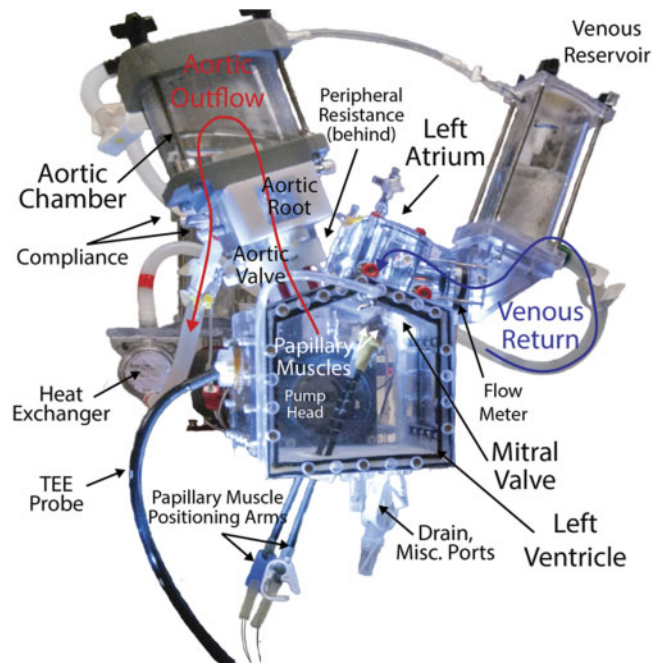


**Figure 1:** Schematic illustration of 3D-printed customized and modular left heart simulator with components labelled. Misc.: miscellaneous; TEE: transoesophageal echocardiography.

(MAP) of 100 mmHg, a systolic pressure of 120 mmHg and a diastolic pressure of 80 mmHg. Normal saline (0.9%) was used as the test fluid for proper conduction and function of the electromagnetic flowmeters.

## Sample preparation

Porcine hearts were obtained from a local abattoir and the complete mitral valve (MV) apparatus, including the chordae tendinae and PM, as well as the annulus and a cuff of left atrial tissue, was dissected free from the surrounding tissue. Valves with inter-commissural distances of 34–36 mm were used. A 3D-printed elastomeric sewing ring was used to mount the valve inside of the LHS by sewing the left atrial cuff to the sewing ring using a continuous suture. Carbon fibre positioning rods with 3D-printed PM holders were used to secure the PM position by sewing them to the holders.

## Study design and experimental setup

The MV was divided into quadrants for analysis according to the PM heads (Fig. 2A) [(i) anterior PM–anterior head (A1–A2 quadrant), (ii) anterior PM–lateral head (P1–P2 quadrant), (iii) posterior PM–posterior head (P2–P3 quadrant) and (iv) posterior PM–medial head (A2–A3 quadrant)]. An incomplete counterbalanced repeated measures design where each valve serves as its own positive and negative control was used. A total of 32 porcine MVs were analysed in the *ex vivo* model. Haemodynamics were first measured in the valve at baseline (healthy pre-rupture, i.e. control valve). Next, MR was induced by cutting primary and secondary chordae from 1 head (quadrant) of interest. The chordae were incrementally cut from 1/3 to the total number of chordae arising from 1 PM head of interest to simulate different extents of rupture and degrees of MR severity (Fig. 2B and Video 1). Measurements were performed following the cut of each third. The experiment was performed 4 times per quadrant, cutting the chordae in a clockwise direction, and was repeated 4 more times per quadrant, cutting the chordae in a counterclockwise direction, thus leading to a total sample size of 32 porcine MVs.

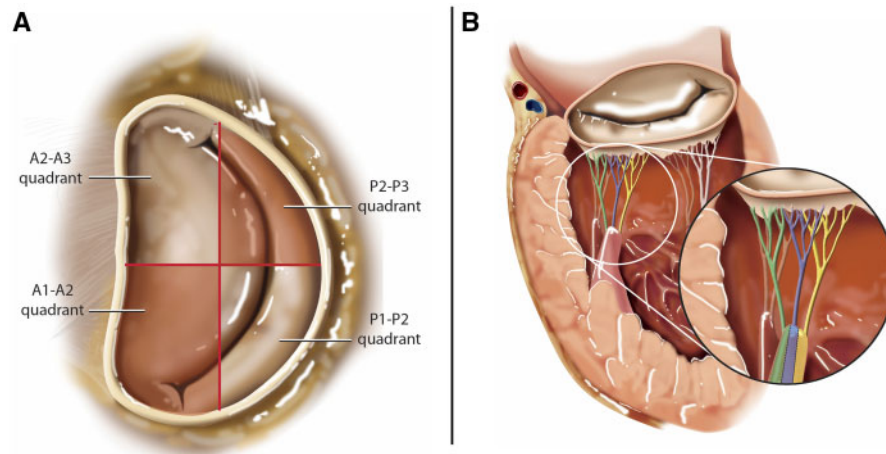


**Figure 2:** Schematic representation of: (A) the mitral valve and its quadrants based on the papillary muscle head's location and (B) cutting pattern by thirds during *ex vivo* acute papillary muscle rupture simulation to recreate partial and full rupture.

## Haemodynamics

Regurgitation fraction (RF), MAP, CO and left atrial pressure (LAP) were precisely measured in the *ex vivo* LHS. However, to provide a more understandable numerical representation of the resulting relative LA pressure increase following chordal rupture, the LA pressure is not reported throughout the manuscript as an absolute value but as a ratio of the LA pressure over the MAP.

## Data acquisition and statistical analysis

Given the inexistence of a previous similar model to simulate PM rupture and the unclear expected effects, statistical power calculations for sample size determination are not accurate for this specific experimental model and were therefore not performed [25–27]. To account for the resulting treatment effect uncertainty, continuous variables are reported as mean and 95% confidence intervals (in parentheses) throughout the manuscript, as suggested by Hickey *et al.* [25].



**Video 1:** Acute papillary muscle rupture disease model using the 3D-printed left heart simulator. This specific example of the experimental setup shows a counterclockwise cutting direction (A3?A2) of chordae from the medial head of the posteromedial papillary muscle, starting with 1/3 rupture and incrementally cutting until full rupture is achieved (to see video: <https://youtu.be/jPdFxe5lvlg>).

Haemodynamic data were recorded with a data acquisition system integrated into the linear pump (ViVitro). MATLAB (MathWorks, Natick, MA, USA) was used for measurement processing. Pairwise comparison of haemodynamic variables according to the rupture site (anterolateral versus posteromedial PMs; Table 1) or rupture direction (clockwise versus counterclockwise; Table 4) was performed using independent two-tailed Student's *t*-test. Non-parametric Friedman tests were performed to compare haemodynamic variables according to the extent of rupture (from baseline to full rupture; Table 2). In addition, a *post hoc* analysis with paired Wilcoxon tests and Bonferroni correction was performed to compare the variables included in the Friedman tests. A comparison of haemodynamic variables among the 4 quadrants was performed using the non-parametric Kruskal-Wallis test (Table 3). A linear regression analysis was performed to evaluate and confirm the haemodynamic variation trend after incremental chordal rupture (from baseline to full rupture). A *P*-value of <0.05 was considered statistically significant for all tests. All tests were performed using R (The R Foundation for Statistical Computing, Austria; Version 4.0.5)

## RESULTS

The incremental chordal cutting by thirds led to a detrimental effect on the haemodynamics in terms of a progressive increase of the measured RF and LA pressure/MAP ratio and a continuous decrease of the MAP and CO (Tables 1–4 and Figs 3 and 4). A *post hoc* analysis comparing the different rupture extents (i.e. the different 'thirds') showed a significant difference in every pairwise comparison of all haemodynamic parameters (RF, CO, MAP) except for the LAP/MAP ratio. Every *post hoc* pairwise comparison of the LAP/MAP ratio was significant except for baseline versus 1/3 rupture and 1/3 rupture versus 2/3 rupture. The chordal cutting direction (i.e. clockwise or counterclockwise) did not influence the haemodynamic changes (Table 4).

Irrespective of the affected quadrant, the rupture of up to 2/3 of the chordae from a given PM head progressively led to a considerable mitral RF but without significant haemodynamic

**Table 1:** Comparison of haemodynamics as a function of the rupture site (anterolateral versus posteromedial papillary muscles)

Extent of rupture	Rupture at anterolateral PM	Rupture at posteromedial PM	<i>P</i> -Value*
Regurgitation fraction (%)			
One-third	27.0 (24.7–29.3)	20.6 (17.7–23.5)	0.050
Two-thirds	43.7 (38.8–48.6)	35.6 (31.3–39.9)	0.105
Full	75.5 (70.2–80.8)	59.1 (51.7–66.5)	0.043
Cardiac output (l/min)			
One-third	3.6 (3.4–3.8)	3.8 (3.6–4.0)	0.194
Two-thirds	2.9 (2.7–3.1)	3.2 (2.9–3.5)	0.214
Full	1.5 (1.2–1.8)	2.3 (1.9–2.6)	0.041
Mean arterial pressure (mmHg)			
One-third	86.9 (85.9–87.9)	94.4 (92.4–96.4)	0.004
Two-thirds	67.9 (60.8–75.0)	86.3 (84.9–87.7)	0.031
Full	34.8 (28.0–41.6)	53.7 (43.9–63.5)	0.051
Left atrial pressure/mean arterial pressure (%)			
One-third	11.9 (11.3–12.5)	11.1 (10.6–11.5)	0.128
Two-thirds	16.4 (13.4–19.4)	13.0 (12.9–13.0)	0.141
Full	33.2 (26.9–39.4)	20.4 (16.6–24.2)	0.045

Continuous variables are expressed as mean and 95% confidence interval in parentheses.

\*Comparisons performed using independent two-tailed Student's *t*-test.

PM: papillary muscle.

**Table 2:** Comparison of haemodynamics as a function of rupture extent

	Baseline	One-third rupture	Two-thirds rupture	Full rupture	P-Value*
Regurgitation fraction (%)	17.2 (15.0–19.4)	23.8 (19.7–27.9)	39.6 (33.3–45.9)	67.3 (59.7–74.9)	<0.001
Cardiac output (l/min)	4.0 (3.8–4.2)	3.7 (3.4–3.8)	3.1 (2.8–3.4)	1.9 (1.4–2.1)	<0.001
MAP (mmHg)	98.1 (96.5–99.7)	90.6 (86.4–94.8)	77.1 (69.5–84.7)	44.2 (35.2–53.2)	<0.001
LAP/MAP (%)	10.6 (10.0–11.2)	11.7 (10.8–12.6)	15.2 (12.2–18.2)	30.1 (23.3–36.9)	<0.001

Continuous variables are expressed as mean and 95% confidence interval in parentheses.

\*Comparisons performed using non-parametric Friedman tests.

LAP: left atrial pressure; MAP: mean arterial pressure.

**Table 3:** Comparison of haemodynamics as a function of rupture site (quadrants)

Extent of rupture	Anterolateral PM		Posteromedial PM		P-Value*
	A1–A2 quadrant (anterior head)	P1–P2 quadrant (lateral head)	P2–P3 quadrant (posterior head)	A2–A3 quadrant (medial head)	
Regurgitation fraction (%)					
One-third	24.7 (15.1–34.3)	29.3 (19.5–39.1)	21.4 (15.0–27.8)	19.8 (13.8–25.8)	0.45
Two-thirds	46.0 (34.6–57.4)	41.2 (27.8–54.6)	35.2 (20.0–50.4)	36.0 (24.6–47.4)	
Full	80.4 (73.0–87.8)	70.7 (57.0–84.4)	60.4 (46.3–74.5)	57.8 (38.4–77.2)	
Cardiac output (l/min)					
One-third	3.7 (3.2–4.2)	3.5 (3.2–3.8)	3.6 (3.2–4.0)	4.0 (3.6–4.4)	0.45
Two-thirds	2.8 (2.3–3.3)	3.0 (2.5–3.5)	3.1 (2.3–3.9)	3.3 (2.9–3.7)	
Full	1.2 (0.7–1.7)	1.7 (1.0–2.4)	2.2 (1.6–2.8)	2.4 (1.5–3.3)	
Mean arterial pressure (mmHg)					
One-third	88.2 (77.4–99.0)	85.6 (74.6–96.6)	94.6 (93.1–100.1)	94.1 (88.5–99.7)	0.44
Two-thirds	64.6 (47.1–82.1)	71.1 (51.9–90.3)	87.9 (83.8–91.9)	84.7 (75.2–94.2)	
Full	30.8 (19.0–42.6)	38.7 (21.7–55.7)	53.7 (33.8–73.6)	53.7 (34.7–72.7)	
Left atrial pressure/mean arterial pressure (%)					
One-third	12.5 (10.0–14.9)	11.8 (10.2–13.4)	11.4 (9.8–13.0)	11.3 (9.7–12.9)	0.36
Two-thirds	19.7 (9.7–29.7)	16.8 (11.4–22.2)	11.5 (9.9–13.1)	12.7 (10.3–15.1)	
Full	39.7 (30.9–48.5)	36.3 (15.1–57.5)	22.5 (16.1–28.9)	22.1 (12.5–31.7)	

Continuous variables are expressed as mean and 95% confidence interval in parentheses.

\*Comparisons performed using non-parametric Kruskal–Wallis tests.

PM: papillary muscle.

**Table 4:** Comparison of haemodynamics as a function of rupture's direction (clockwise versus counterclockwise)

Extent of rupture	Anterolateral PM		P-Value	Posteromedial PM		P-Value*
	Clockwise cutting	Counterclockwise cutting		Clockwise cutting	Counterclockwise cutting	
Regurgitation fraction (%)						
One-third	27.5 (27.0–27.9)	26.5 (20.9–32.1)	0.82	20.1 (14.3–25.9)	21.1 (17.0–25.2)	0.92
Two-thirds	37.2 (36.8–37.6)	50.2 (44.4–56.0)	0.26	37.1 (30.2–43.9)	34.2 (26.5–41.9)	0.24
Cardiac output (l/min)						
One-third	3.7 (3.5–3.9)	3.5 (3.2–3.8)	0.54	3.9 (3.4–4.4)	3.8 (3.6–3.9)	0.93
Two-thirds	3.2 (3.1–3.3)	2.7 (2.6–2.8)	0.061	3.1 (2.5–3.7)	3.4 (3.0–3.8)	0.42
Mean arterial pressure (mmHg)						
One-third	86.5 (84.3–88.7)	87.4 (86.7–88.1)	0.63	97.1 (95.8–98.4)	91.6 (89.8–93.4)	0.31
Two-thirds	76.0 (72.2–79.8)	59.8 (48.8–70.8)	0.44	84.9 (83.5–86.3)	87.8 (85.6–90.0)	0.24
Left atrial pressure/mean arterial pressure (%)						
One-third	11.1 (11.0–11.2)	12.7 (12.1–13.3)	0.12	10.4 (10.3–10.5)	11.8 (11.7–11.9)	0.021
Two-thirds	13.4 (11.6–15.2)	19.5 (14.4–24.6)	0.53	13.0 (12.3–13.7)	13.0 (12.6–13.4)	1.00

Continuous variables are expressed as mean and 95% confidence interval in parentheses.

\*Comparisons performed using independent two-tailed Student's *t*-test.

PM: papillary muscle.

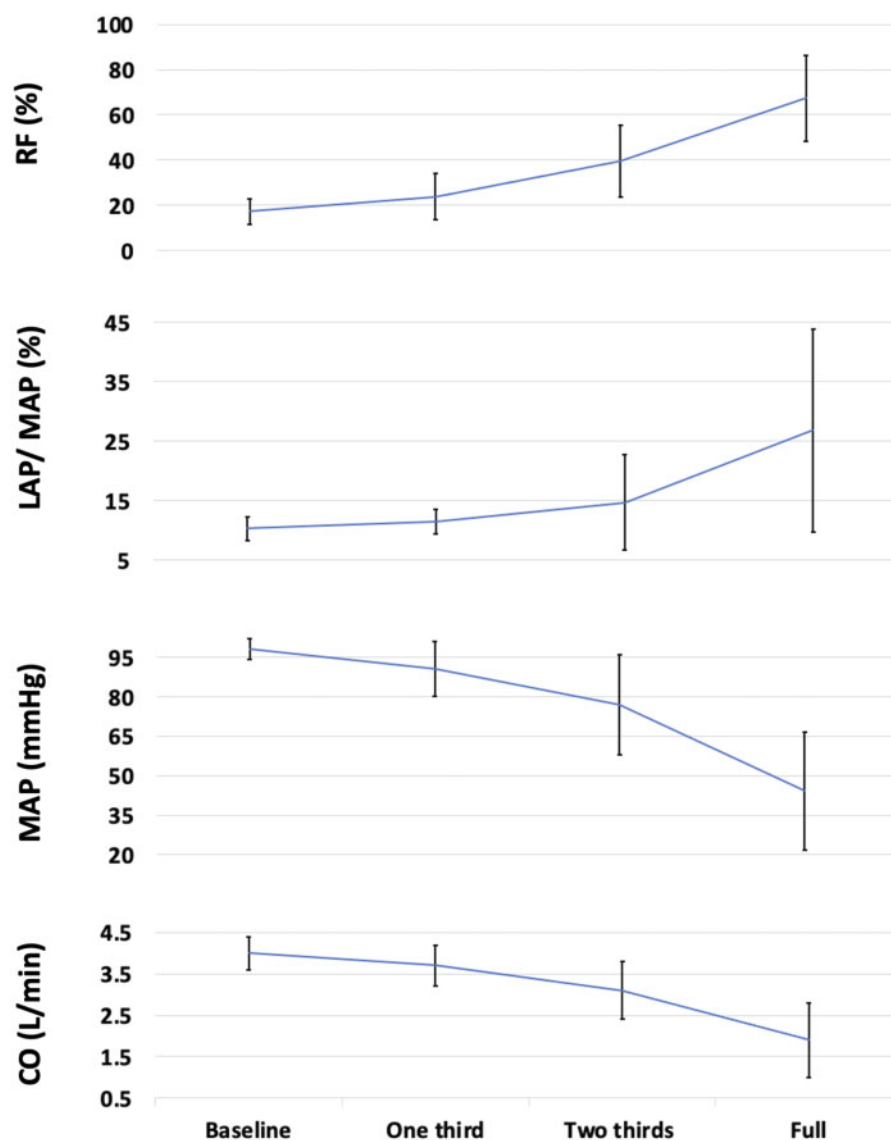


**Figure 3:** Haemodynamic changes according to the extent of rupture expressed as mean value  $\pm$  standard deviation for all 4 quadrants. The lines represent the mean values of the different haemodynamic parameters according to the extent of rupture (ranging from 1/3 to full rupture). Haemodynamics compatible with cardiogenic shock are only observed after a regurgitation fraction threshold of 60% is exceeded. CO: cardiac output; LAP: left atrial pressure; MAP: mean arterial pressure; RF: regurgitation fraction.

effects. A complete chordal rupture (i.e.  $>2/3$ ) led to severe MR with markedly reduced subsequent haemodynamic parameters indicative of CS (Fig. 3). As a clinical surrogate of rupture extent, RF  $>60\%$  led to haemodynamics compatible with CS (Tables 1–3 and Figs 3 and 4). Regression analysis showed a statistically significant ( $P < 0.001$ ) linear effect on haemodynamics after incremental PM rupture. Per every third rupture increase, the mean RF increased 16.6% (14.0–19.2%) and the mean LAP/MAP increased 6.0% (4.0–8.0%). The mean CO decreased 0.7 l/min (0.6–0.8 l/min) and the mean MAP decreased 17.5 mmHg (14.5–20.6 mmHg).

Rupture occurring at the anterolateral PM (i.e. A1–A2 and P1–P2 quadrants) had a considerably more pronounced negative effect on haemodynamics than rupture at the posteromedial PM (Fig. 4A and Table 1). In addition, a differentiated analysis per quadrant showed that rupture occurring in the A1–A2 quadrant (anterior head of the anterolateral PM) led to more marked

haemodynamic instability compared to the other quadrants (Fig. 4B and Table 3).

## DISCUSSION

This bioengineering-based study analyses an acute PM rupture disease model based on *ex vivo* simulation with a previously validated LHS [16–24]. The experimental setup was designed to study different PM rupture variations in terms of location and extent of the rupture. To the best of our knowledge, this is the first experimental study of this type, creating an acute PM rupture disease model to increase the understanding of this lethal disease. The main findings of the study are:

1. The severity of the haemodynamic changes following acute PM rupture varies considerably according to the site and extent of the rupture.

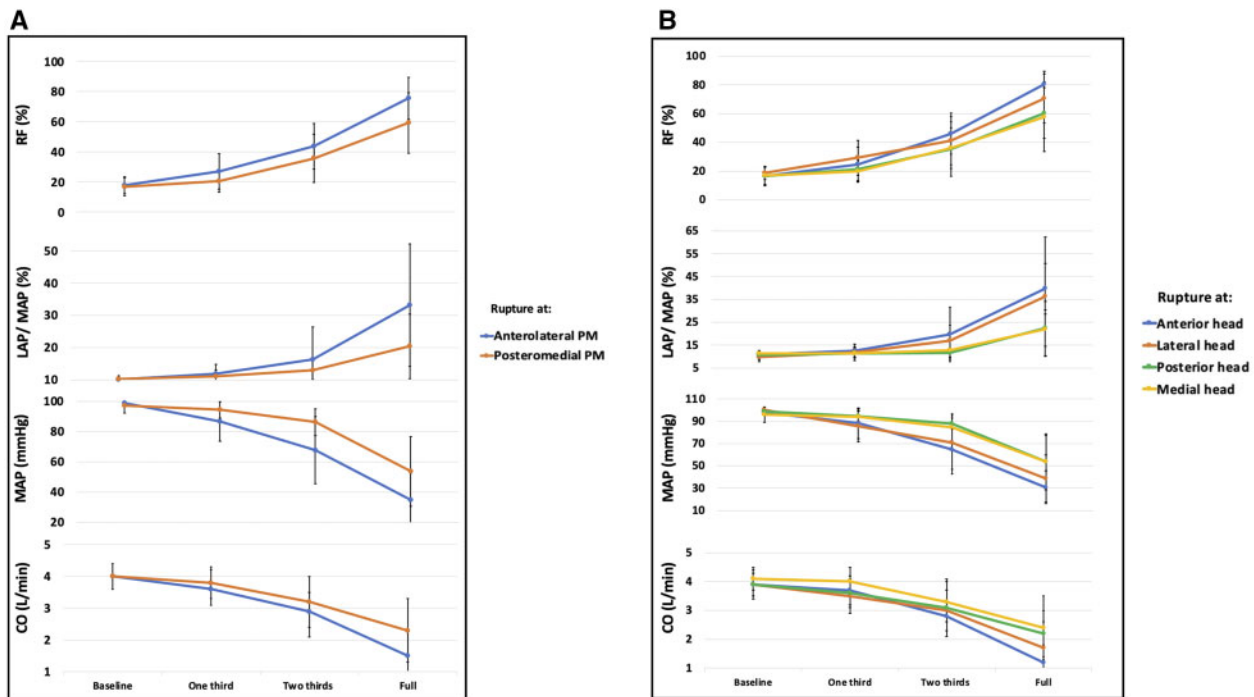


**Figure 4:** Haemodynamic changes according to the extent of rupture expressed as mean value  $\pm$  standard deviation: **(A)** comparison of both papillary muscles and **(B)** comparison among the 4 papillary muscle heads. According to the colour code and the extent of rupture (ranging from 1/3 to full rupture), the lines represent the mean values of the different haemodynamic parameters given the rupture at a specific papillary muscle or head. Haemodynamics compatible with cardiogenic shock are only observed after a regurgitation fraction threshold of 60% is exceeded. CO: cardiac output; LAP: left atrial pressure; MAP: mean arterial pressure; PM: papillary muscle; RF: regurgitation fraction.

- Rupture of  $\leq 2/3$  of the chordae tendineae from 1 PM head or rupture occurring at 1 head from the posteromedial PM leads to less severe haemodynamic deterioration.
- Rupture occurring at the anterolateral PM, specifically the anterior head,  $>2/3$  rupture of the chordae tendineae from 1 PM head or RF  $>60\%$  lead to marked haemodynamic instability.

Acute PM rupture is a dreaded mechanical complication frequently associated with poor clinical outcomes, given the impact of the resulting severe acute MR on haemodynamics. The known poor clinical outcomes, the broad spectrum of clinical presentations and lack of data on patient selection and timing strategies make this patient group particular unappealing for most cardiac surgeons. In addition, the preoperative patient risk may be underestimated in some patients because of the overestimation of left ventricular function in patients with acute MR. In this regard, we believe an *ex vivo* model of this perplexing and highly lethal clinical entity would be of interest to the cardiac surgery community.

An experimental *ex vivo* disease model may increase our understanding of acute PM rupture, possibly changing the previous paradigm by shifting the definition of this clinical scenario from a 'binary' to a 'spectral' understanding of the disease depending on the specific rupture's location and extent. For example, according to our observed results, the haemodynamic effects are markedly different if the rupture occurs at the anterolateral or the posteromedial PM. Similarly, the extent of the rupture has a significant influence on the severity of the acute effects. For example, the rupture of a complete PM head leads to catastrophic haemodynamic parameters. Still, the rupture of only one-third of the chordae arising from 1 PM head may have a very benign clinical presentation with mild haemodynamic consequences.

The clinical translation of these results could help the clinician improve preoperative decision-making and patient selection, thus potentially improving clinical outcomes. However, the translation and applicability of these results to a clinical scenario strongly depend on high-quality cardiac imaging describing the exact PM rupture characteristics. Hence, we advise avoiding the general term 'acute PM rupture' in diagnostic imaging test reports (e.g. echocardiography) and instead characterize the rupture more descriptively in terms of site and extent.

Following this rationale, the concept of PM rupture 'spectrum' helps classify patients and make surgical eligibility and timing decisions. Based on our results, we hypothesize that patients presenting with rupture of the posteromedial PM or  $\leq 2/3$  of the chordae from 1 PM head are better surgical candidates since they will more likely tolerate surgery due to less affected preoperative haemodynamics. On the other hand, we hypothesize that patients presenting with acute PM rupture of  $>2/3$  of the chordae tendineae from a PM head, rupture of the anterolateral PM, specifically the anterior PM head, or RF  $>60\%$  are more likely to develop severe haemodynamic alterations and might benefit from bridging strategies such as temporary MCS before undergoing corrective surgery.

Predicting the severity of the haemodynamic decompensation based on our *ex vivo* simulation results may not only be useful in helping to identify the need for temporary MCS but may also help surgeons to design a surgical plan in terms of intraoperative timing for cannulation and coronary graft harvesting and to consider either MV replacement or repair. A successful MV repair is more likely in patients presenting with a less decompensated haemodynamic state and less extensive rupture (e.g. partial PM/chordal rupture), particularly in patients who are operated on later in the disease process when PM tissues are less friable [28].

Since the most common cause of acute PM is MI [1–3], the regional myocardial coronary blood supply has an important influence on the rupture location. As observed in this study, rupture occurring at the posteromedial PM leads to less severe haemodynamic consequences than the anterolateral PM. Acute rupture is more likely to occur in a PM with a single-vessel coronary blood supply [29, 30]. Hence, acute PM rupture occurs more frequently at the posteromedial PM because its coronary blood supply arises solely from the right coronary artery in most patients. In contrast, the anterolateral PM has a combined coronary blood supply provided by the left anterior descending and circumflex arteries. Hence, even if the acute rupture of the posteromedial PM has a higher incidence, the deleterious effects on the function of the MV and the negative haemodynamic consequences are less severe.

Although we demonstrated a statistically significant difference when comparing the haemodynamic changes following anterolateral or posteromedial PM rupture, we failed to find such differences according to specific quadrant rupture location. Nonetheless, despite the absence of statistical significance, the observed total numerical difference among quadrants has clinical relevance. For example, when comparing the A1–A2 and A2–A3 quadrants, the observed differences after full rupture were ~22%, 23 mmHg and 1.2 l/min in the measured RF, MAP and CO, respectively. These differences observed among quadrants might be explained by an unequal proportion of chordae tendineae arising from each PM head and asymmetrical distribution of chordae along the mitral leaflets. During valve preparation, we observed that chordae arising from the anterolateral PM, especially from the anterior head, are responsible for a wider mitral leaflet area compared to the other PM heads, thus explaining why rupture of the same extent at the anterior PM head leads to a more severe MR and therefore worse haemodynamics.

A wide variety of concomitant factors need to be considered in a patient-specific decision-making process when considering surgery for acute PM. However, we believe that the observations from our *ex vivo* study may further help clinicians guide their difficult decision-making processes for these high-risk, complex patients.

## Limitations

While the *ex vivo* experimental setup used in this study is a reliable, reproducible and controllable method to study the haemodynamics and biomechanics of the MV, there are limitations to this approach. First, the model does not perfectly simulate the physiological interactions between the annulus and ventricle. In addition, the employed valves were normal MVs from healthy pigs and severe MR was induced by cutting chordae rather than through native pathological processes, resulting in chordal rupture. Second, the most common aetiology of PM rupture is the ACS that results in MI. The *ex vivo* model is unable to completely simulate the additional consequences of MI, such as ventricular dysfunction or cardiac arrhythmias. Therefore, the observed deteriorated haemodynamics result from the dysfunctional MV and the resulting severe MR. Nonetheless, this last aspect can also be seen as a strength since it eliminates these confounding variables, thus focusing the observations on the MV apparatus. Third, normal anatomical variations of the PM in terms of different degrees of fusion or separation of the PM heads have been described [31]. These variations can lead to a different biomechanical behaviour of the MV after acute PM rupture leading to effects on the haemodynamics that might differ from patient to patient and even from the results obtained with our *ex vivo* model. However,

it was not possible to include anatomical variations in our experimental design. Finally, the use of porcine valves rather than human MVs is an intrinsic limitation. However, porcine valves are strikingly similar to human valves in terms of the leaflet, annular and PM anatomies as well as chordae distribution, density and cellular composition [32, 33].

## CONCLUSION

The haemodynamic effects of acute PM rupture vary considerably according to the site and extent of the rupture. Rupture of  $\leq 2/3$  of chordae from 1 PM head or rupture of the posteromedial PM lead to less marked haemodynamic effects, suggesting a more benign clinical presentation and a higher likelihood of surgery tolerance in patients presenting with this clinical scenario. Rupture of the anterolateral PM, specifically the anterior head, rupture of  $>2/3$  of chordae from 1 PM head, or RF  $>60\%$  lead to marked haemodynamic instability, suggesting that patients in this clinical scenario might benefit from bridging strategies prior to surgery. A differentiated understanding of the acute PM rupture spectrum can improve preoperative decision-making and patient selection.

## Funding

This work was supported by the National Institutes of Health (NIH R01 HL152155 and NIH R01 HL089315-01, Y. Joseph Woo), the Thoracic Surgery Foundation Resident Research Fellowship (Yuanjia Zhu), the National Science Foundation Graduate Research Fellowship Program (DGE-1656518, Annabel M. Imbrie-Moore) and a Stanford Graduate Fellowship (Annabel M. Imbrie-Moore). We thank Donald and Sally O'Neal for their generous donation and support of this project. The content is solely the authors' responsibility and does not necessarily represent the official views of the funders.

**Conflict of interest:** Michael A. Borger discloses that his hospital receives speakers' honoraria and/or consulting fees on his behalf from Edwards Lifesciences, Medtronic, Abbott, and CryoLife. The remaining authors have no conflicts of interest or financial relationships with the industry to disclose.

## Author contributions

**Mateo Marin-Cuartas:** Conceptualization; Formal analysis; Investigation; Methodology; Project administration; Visualization; Writing—original draft; Writing—review & editing. **Yuanjia Zhu:** Formal analysis; Methodology; Writing—review & editing. **Annabel M. Imbrie-Moore:** Formal analysis; Methodology; Writing—review & editing. **Matthew H. Park:** Formal analysis; Methodology; Writing—review & editing. **Robert J. Wilkerson:** Data curation; Investigation; Software. **Matthew Leipzig:** Formal analysis; Validation; Statistics. **Pearly K. Pandya:** Formal analysis; Writing—review & editing. **Michael J. Paulsen:** Methodology; Writing—review & editing. **Michael A. Borger:** Funding acquisition; Resources; Validation; Writing—review & editing. **Y. Joseph Woo:** Formal analysis; Funding acquisition; Methodology; Resources; Supervision; Validation; Writing—review & editing.

## Reviewer information

Interactive CardioVascular and Thoracic Surgery thanks Vito Domenico Bruno, Ari Mennander and the other, anonymous reviewer(s) for their contribution to the peer review process of this article.

## REFERENCES

- [1] Pahuja M, Ranka S, Chauhan K, Patel A, Chehab O, Elmoghrabi A, *et al.* Rupture of papillary muscle and chordae tendinae complicating STEMI: a call for action. *ASAIO J* 2021;67:907-916.
- [2] Kilic A, Sultan I, Chu D, Wang Y, Gleason TG. Mitral valve surgery for papillary muscle rupture: outcomes in 1342 patients from the Society of Thoracic Surgeons Database. *Ann Thorac Surg* 2020;110:1975-1981.
- [3] Fujita T, Yamamoto H, Kobayashi J, Fukushima S, Miyata H, Yamashita K, *et al.* Mitral valve surgery for ischemic papillary muscle rupture: outcomes from the Japan cardiovascular surgery database. *Gen Thorac Cardiovasc Surg* 2020;68:1439-1446.
- [4] Schroeter T, Lehmann S, Misfeld M, Borger M, Subramanian S, Mohr FW, *et al.* Clinical outcome after mitral valve surgery due to ischemic papillary muscle rupture. *Ann Thorac Surg* 2013;95:820-4.
- [5] Wei JY, Hutchins GM, Bulkley BH. Papillary muscle rupture in fatal acute myocardial infarction: A potentially treatable form of cardiogenic shock. *Ann Intern Med* 1979;90:149-152.
- [6] Thompson CR, Buller CE, Sleeper LA, Antonelli TA, Webb JG, Jaber WA, *et al.* Cardiogenic shock due to acute severe mitral regurgitation complicating acute myocardial infarction: a report from the SHOCK Trial Registry. Should we use emergently revascularize Occluded Coronaries in cardiogenic shock? *J Am Coll Cardiol* 2000;36:1104-9.
- [7] Russo A, Suri RM, Grigioni F, Roger VL, Oh JK, Mahoney DW, *et al.* Clinical outcome after surgical correction of mitral regurgitation due to papillary muscle rupture. *Circulation* 2008;118:1528-34.
- [8] Atreya AR, Kawamoto K, Yelavarthy P, Arain MA, Cohen DG, Wanamaker BL, *et al.* Myocardial infarction and papillary muscle rupture in the COVID-19 era. *JACC Case Rep* 2020;2:1637-1641.
- [9] Kunkel KJ, Anwaruddin S. Papillary muscle rupture due to delayed STEMI presentation in a patient self-isolating for presumed COVID-19. *JACC Case Rep* 2020;2:1633-1636.
- [10] Ushioda R, Fujii A, Shirakawa M, Shirasaka T, Kikuchi S, Kamiya H, *et al.* Ventricular septal perforation followed by papillary muscle rupture with acute myocardial infarction: efficacy of venoarterial extracorporeal membrane oxygenation. *J Surg Case Rep* 2020.
- [11] Pinto R, Maia R, Pinho P, Roncon-Albuquerque R Jr. Perioperative extracorporeal membrane oxygenation for refractory cardiopulmonary failure complicating papillary muscle rupture. *Heart Lung Circ* 2021;30:303-309.
- [12] Kaku Y, Nakano J, Pham DT. Successful support of cardiogenic shock due to a ruptured papillary muscle using an Impella 5.0. *Artif Organs* 2020;44:900-901.
- [13] Bahlmann E, Frerker C, Kreidel F, Thielsen T, Ghanem A, van der Schalk H, *et al.* MitraClip implantation after acute ischemic papillary muscle rupture in a patient with prolonged cardiogenic shock. *Ann Thorac Surg* 2015;99:e41-2.
- [14] Papadopoulos K, Chrissoheris M, Nikolaou I, Spargias K. Edge-to-edge mitral valve repair for acute mitral valve regurgitation due to papillary muscle rupture: a case report. *Eur Heart J Case Rep* 2019;3(1):ytz001.
- [15] Vo TX, Chan V, Ruel M. Surgery for mitral valve papillary muscle rupture: implications of replacement versus repair. *Ann Thorac Surg* 2020;110:1982.
- [16] Paulsen MJ, Kasinpila P, Imbrie-Moore AM, Wang H, Hironaka CE, Koyano TK, *et al.* Modeling conduit choice for valve-sparing aortic root replacement on biomechanics with a 3-dimensional-printed heart simulator. *J Thorac Cardiovasc Surg* 2019;158:392-403.
- [17] Paulsen MJ, Imbrie-Moore AM, Baiocchi M, Wang H, Hironaka CE, Lucian HJ, *et al.* Comprehensive ex vivo comparison of 5 clinically used conduit configurations for valve-sparing aortic root replacement using a 3-dimensional-printed heart simulator. *Circulation* 2020;142:1361-1373.
- [18] Paulsen MJ, Bae JH, Imbrie-Moore AM, Wang H, Hironaka CE, Farry JM, *et al.* Development and ex vivo validation of novel force-sensing neo-chordae for measuring chordae tendineae tension in the mitral valve apparatus using optical fibers with embedded Bragg gratings. *J Biomech Eng* 2020;142(1):0145011-9.
- [19] Paulsen MJ, Imbrie-Moore AM, Wang H, Bae JH, Hironaka CE, Farry JM, *et al.* Mitral chordae tendineae force profile characterization using a posterior ventricular anchoring neo-chordal repair model for mitral regurgitation in a three-dimensional-printed ex vivo left heart simulator. *Eur J Cardiothorac Surg* 2020;57:535-544.
- [20] Imbrie-Moore AM, Paulsen MJ, Zhu Y, Wang H, Lucian HJ, Farry JM, *et al.* A novel cross-species model of Barlow's disease to biomechanically analyze repair techniques in an ex vivo left heart simulator. *J Thorac Cardiovasc Surg* 2021;161:1776-1783.
- [21] Imbrie-Moore AM, Paullin CC, Paulsen MJ, Grady F, Wang H, Hironaka CE, *et al.* A novel 3D-printed preferential posterior mitral annular dilation device delineates regurgitation onset threshold in an ex vivo heart simulator. *Med Eng Phys* 2020;77:10-18.
- [22] Imbrie-Moore AM, Paulsen MJ, Thakore AD, Wang H, Hironaka CE, Lucian HJ, *et al.* Ex vivo biomechanical study of apical versus papillary neo-chordal anchoring for mitral regurgitation. *Ann Thorac Surg* 2019;108:90-97.
- [23] Zhu Y, Imbrie-Moore AM, Paulsen MJ, Priromprintr B, Wang H, Lucian HJ, *et al.* Novel bicuspid aortic valve model with aortic regurgitation for hemodynamic status analysis using an ex vivo simulator. *J Thorac Cardiovasc Surg* 2020 Jun 29:S0022-5223(20)31749-9.
- [24] Zhu Y, Imbrie-Moore AM, Paulsen MJ, Priromprintr B, Park MH, Wang H, *et al.* Regurgitation model from cusp prolapse with hemodynamic validation using an ex vivo left heart simulator. *J Cardiovasc Transl Res* 2021;14:283-289.
- [25] Hickey GL, Grant SW, Dunning J, Siepe M. Statistical primer: sample size and power calculations-why, when and how? *Eur J Cardiothorac Surg* 2018;54:4-9.
- [26] Kraemer HC, Mintz J, Noda A, Tinklenberg J, Yesavage JA. Caution regarding the use of pilot studies to guide power calculations for study proposals. *Arch Gen Psychiatry* 2006;63:484-9.
- [27] Hoening JM, Heisey DM. The abuse of power: the pervasive fallacy of power calculations for data analysis. *Am Stat* 2001;55:19-24.
- [28] Bouma W, Wijdh-den Hamer IJ, Klinkenberg TJ, Kuijpers M, Bijleveld A, van der Horst IC, *et al.* Mitral valve repair for post-myocardial infarction papillary muscle rupture. *Eur J Cardiothorac Surg* 2013;44:1063-9.
- [29] Nishimura RA, Schaff HV, Shub C, Gersh BJ, Edwards WD, Tajik AJ. Papillary muscle rupture complicating acute myocardial infarction: analysis of 17 patients. *Am J Cardiol* 1983;51:373-7.
- [30] Voci P, Bilotta F, Caretta Q, Mercanti C, Marino B. Papillary muscle perfusion pattern. A hypothesis for ischemic papillary muscle dysfunction. *Circulation* 1995;91:1714-8.
- [31] Nappi F, Spadaccio C, Acar C. A surgical perspective on ischemic mitral regurgitation: tethering or prolapse? Going back to papillary muscles anatomy. What the surgeons really need to know. *World J Cardiovasc Surg* 2015;7:63-69.
- [32] Crick SJ, Sheppard MN, Ho SY, Gebstein L, Anderson RH. Anatomy of the pig heart: comparisons with normal human cardiac structure. *J Anat* 1998;193:105-119.
- [33] Millington-Sanders C, Meir A, Lawrence L, Stolinski C. Structure of chordae tendineae in the left ventricle of the human heart. *J Anat* 1998;192:573-581.